molecules

MDPI

*Review*

# Redox Species of Redox Flow Batteries: A Review

**Feng Pan and Qing Wang ***

Received: 16 October 2015 ; Accepted: 9 November 2015 ; Published: 18 November 2015
Academic Editors: Derek J. McPhee and Sergei Manzhos

Department of Materials Science and Engineering, National University of Singapore, Singapore 117575, Singapore; panfeng@u.nus.edu
* Correspondence: qing.wang@nus.edu.sg; Tel.: +65-6516-7118

**Abstract:** Due to the capricious nature of renewable energy resources, such as wind and solar, large-scale energy storage devices are increasingly required to make the best use of the renewable power. The redox flow battery is considered suitable for large-scale applications due to its modular design, good scalability and flexible operation. The biggest challenge of the redox flow battery is the low energy density. The redox active species is the most important component in redox flow batteries, and the redox potential and solubility of redox species dictate the system energy density. This review is focused on the recent development of redox species. Different categories of redox species, including simple inorganic ions, metal complexes, metal-free organic compounds, polysulfide/sulfur and lithium storage active materials, are reviewed. The future development of redox species towards higher energy density is also suggested.

**Keywords:** redox flow battery; redox species; energy density

## 1. Introduction

To meet the energy demands for the increasing global population, the present energy production of the world will be doubled by 2050 [1]. Our society is more aware than ever before of sustainability issues. Due to limited fossil fuel resources and global climate change, the energy increase must be achieved without dramatic $CO_2$ emissions [2]. Under this goal, renewable energy technologies have been popular topics in recent decades. Renewable energy sources, such as wind, solar and tidal, are all generally dispersed and inherently intermittent [3]. Due to the capricious nature of renewable power, advanced large-scale energy storage devices are required to make the best use of these renewable energy resources. However, the present energy storage capacity can only store around 1% of the energy consumed worldwide [1], and the current trend seems to be requiring more energy storage devices at the grid scale to increase the penetration of renewable energy.

Rechargeable batteries offer an efficient way to store energy. Available battery technologies include lithium ion, nickel-metal hydride (Ni-MH), lead acid, redox flow and the sodium-sulfur (Na-S) system. Among them, the redox flow battery (RFB) is considered a promising energy-storage solution, which is suitable for stationary applications due to its modular design, good scalability, flexible operation and moderate maintenance cost [4]. RFB systems possess a unique structure, which consists of three parts: stack cell, energy storage tanks and the flow system (Figure 1). Unlike the enclosed configuration of lithium ion batteries where energy is stored with the electrode sheets, redox flow batteries employ active species dissolved in the liquid electrolytes, which are stored in the tanks, separated from the electrodes [5]. Upon operating, the fluids (catholyte and anolyte) containing redox active species are driven by the pump and circulate through each of the half compartments of the cells. The conversion between chemical energy and electrical energy occurs while the electrolytes are flowing through the electrodes [6]. Such a configuration brings RFB the most unique and attractive feature that other battery systems do not have: decoupled energy storage and power generation,

which enables an independent control of capacity and power to meet different requirements ranging from a few kWh to several MWh.

The redox flow battery has been developed for large-scale application for decades, and some of the RFB systems have been successfully demonstrated at the megawatt scale. However, none of the present systems are widely commercialized. The most severe challenge for RFB is the low energy density, which results in a high cost for unit energy storage. For instance, the energy density of state-of-the-art vanadium-based RFB is in the range of 20–30 $Wh \cdot L^{-1}$, which is much lower than other battery systems, such as lithium ion batteries [7]. Moreover, compared to lithium ion batteries, whose energy density was enhanced by 8%–9% per year since the 1990s [8], the major systems in the RFB field have remained almost the same for more than two decades [9].

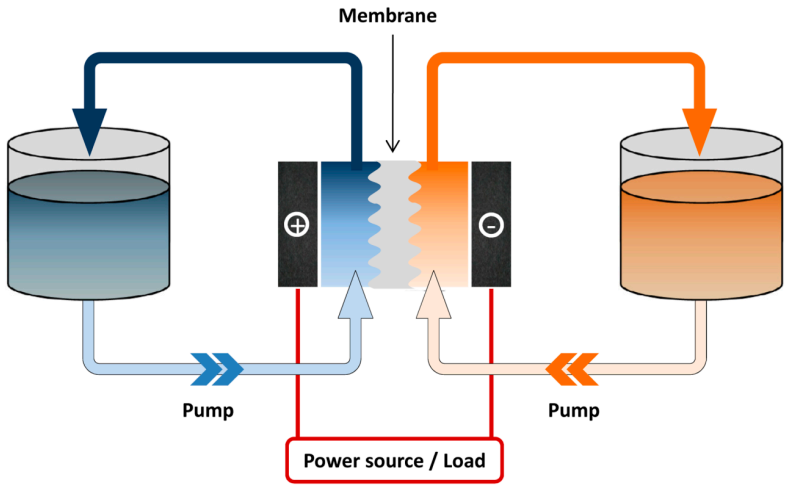


**Figure 1.** Schematic illustration of a redox flow battery. Active species are stored externally in the storage tanks, while the conversion between electrical and chemical energy occurs in the cell unit.

The redox active species is the most important component in redox flow batteries, which dictates the overall performance. From the perspective of energy density, the most important characteristics are redox potential and solubility. The cell voltage is determined by the equilibrium potentials of active species in the cathodic and anodic half-cells, while the capacity is dependent on the effective concentration, which is the solubility multiplied by the number of electrons transferred in the redox reactions [5,10]. Here, we provide an overview of the recent studies on redox species and the development of a redox flow battery. In traditional aqueous RFB systems, the redox species are mostly limited within the category of transition metal ions and halogen ions. In recent year, the non-aqueous system has become a hotspot, because it provides a wider electrochemical window, which further allows for more redox species, like various organic compounds, to be employed. Meanwhile, molecular engineering is being applied to modify those redox couples towards higher solubility and more suitable redox potential. In addition, there have been several new approaches combining RFB with the lithium ion battery concept.

We noticed that several comprehensive reviews have been published in the past few years. Ponce de leon *et al*. discussed the fundamental aspects of different kinds of RFB [11]. The reviews by Skyllas-Kazacos *et al*. and by Alotto *et al*. discussed the technology, application and commercialization status of RFB [4,7]. Zhang *et al*. reviewed the ion exchange membrane in a vanadium redox flow battery [12], while Shin *et al*. gave an overview of membranes for a non-aqueous flow battery [13]. A review by Weber *et al*. discussed the transport and kinetic behaviors on electrode reactions [6]. Leung *et al*. provided a summary of RFB chemistries, design considerations and modeling and applications [14]. Wang *et al*. gave a brief review of the features and progress of the Li-ion and redox flow battery systems and discussed the concept of the Li-redox flow battery [15]. More recently, Wang

*et al*. reviewed the progress of RFB, including cell-level chemistry, electrodes and membranes [9]. Most of them are focused on cell-scale chemistry. Here, we present a review focused on the redox species of redox flow batteries. With an overview of different categories of redox species, a trend towards future higher energy density can be suggested.

## 2. Simple Inorganic Ions

The early research on the redox flow battery was mostly based on metal ions and halogen ions. The simple chemistry and high solubility makes metal ions the most popular candidates for aqueous redox flow batteries. On the other hand, halogens are intensively researched as cathodic active species owing to their high solubility, reversible redox reactions at high potentials and relatively low molecular weight. The most studied halogens, bromine and iodine, show redox potentials within the potential range of water electrolysis. The recent development of aqueous RFB involves a wider range of redox species. Most of them still fall in the category of transition metal ions and halogen ions, such as $VCl_3/VCl_2$, $Br^-/ClBr^{2-}$ [16], $Ce^{3+}/Ce^{4+}$ [17], $Mn^{2+}/Mn^{3+}$ [18], $Ti^{3+}/Ti^{4+}$ [19], $Cu/Cu^{1+}$, $Cu^{1+}/Cu^{2+}$ [20,21], and others [22]. A summary of simple inorganic ions redox species is shown in Table 1. The concentrations displayed here are based on the demonstrated flow cells.

### *2.1. Iron/Chromium*

The first modern redox flow battery was the Fe/Cr system primarily developed at NASA. The $Fe^{3+}/Fe^{2+}$ and $Cr^{3+}/Cr^{2+}$ redox couples were employed in the cathodic and anodic electrolytes, delivering a cell voltage of 1.18 V [23,24].

$$\text{Cathodic: } Fe^{3+} + e^- \leftrightarrow Fe^{2+} \text{ 0.77 V } vs. \text{ standard hydrogen electrode (SHE)} \quad (1)$$

$$\text{Anodic: } Cr^{2+} - e^- \leftrightarrow Cr^{3+} \text{ } - 0.41 \text{ V } vs. \text{ SHE} \quad (2)$$

The $Fe^{3+}/Fe^{2+}$ redox couple shows good reversibility and fast kinetics. However, the slow kinetics of $Cr^{3+}/Cr^{2+}$ usually requires an elevated operation temperature, which significantly increases the cost [25]. Meanwhile, the low redox potential of $Cr^{3+}/Cr^{2+}$ may cause $H_2$ evolution, which limits the Coulombic efficiency and cycle life.

### *2.2. All-Vanadium*

The vanadium redox flow battery (VRB) was first proposed in 1980s by Skyllas-Kazacos and co-workers [26]. Vanadium has four valence states to form two redox couples, $V^{2+}/V^{3+}$ and $VO_2{}^{+}/VO^{2+}$. VRB employs vanadium as the only element in both the catholyte and anolyte, giving a cell voltage of about 1.26 V in 2.0 M $H_2SO_4$ solution [27]. The single compound configuration controls the crossover contamination, which allows a long system life of about 15–20 years [28].

$$\text{Cathodic: } VO_2{}^{+} + 2H^+ + e^- \leftrightarrow VO^{2+} + H_2O \text{ 1.00 V } vs. \text{ SHE} \quad (3)$$

$$\text{Anodic: } V^{2+} - e^- \leftrightarrow V^{3+} \text{ } - 0.26 \text{ V } vs. \text{ SHE} \quad (4)$$

The all-vanadium flow battery is the most extensively-researched redox flow battery technology, and some VRB demonstration systems at the MWh scale have been installed [29–31]. The concentration of vanadium species is around 2.0 M in acidic aqueous electrolytes, and the energy density is 20–30 Wh$\cdot$ L$^{-1}$. Although it seems to have advantages over other flow battery systems, such a low energy density makes it less attractive when compared to rivals, the like lithium ion battery, and this is also the biggest barrier for commercialization. Meanwhile, the toxicity hazard of soluble vanadium and the strong corrosive strength of $VO_2{}^{+}/VO^{2+}$ also hinder the widespread adoption of VRB [32]. Various modifications have been proposed based on vanadium redox flow battery chemistry [33]. For instance, researchers from the Pacific Northwest National Laboratory

(PNNL) reported a Fe/V battery, combining the advantages of the Fe/Cr system and VRB, while avoiding their drawbacks, such as the slow kinetics of $Cr^{3+}/Cr^{2+}$ and the high corrosive strength of $VO_2^{+}/VO^{2+}$ [34]. Meanwhile, researchers from the University of Twente reported a new concept of a vanadium/air battery with $V^{3+}/V^{2+}$ as the anodic redox couple and $H_2O/O_2$ as the cathodic redox couple [35,36].

### 2.3. Vanadium/Bromine

The vanadium-bromine battery employs $VBr_3/VBr_2$ and $Br^-/ClBr^-$ in the anolyte and catholyte, respectively, with HBr and HCl as the supporting electrolyte [29].

$$\text{Cathodic: } 2Br^- + Cl^- \leftrightarrow ClBr_2^- + 2e^- \ 1.09 \text{ V } vs. \text{ SHE} \quad (5)$$

$$\text{Anodic: } 2VBr_3 + 2e^- \leftrightarrow 2VBr_2 + 2Br^- \ -0.26 \text{ V } vs. \text{ SHE} \quad (6)$$

The higher solubility of vanadium bromine (1.0–3.0 M) than vanadium sulfate increases the energy density. One disadvantage of the vanadium/bromine system is the possible $Br_2$ vapor emission [29].

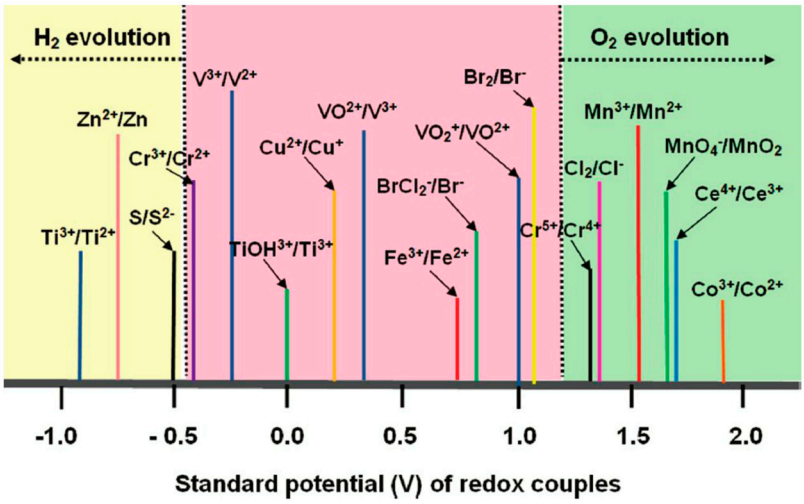


**Figure 2.** Redox potentials (*vs.* standard hydrogen electrode) of various redox couples (reproduced with permission from Chem Rev 111, 3577–3613 (2011); Copyright 2011, American Chemical Society).

### 2.4. Zinc/Bromine

The Zn-Br battery (ZBB) is another successful redox flow battery system, which has been demonstrated for decades [37]. The cathodic reaction involves the reduction of $Br_2$ and oxidation of $Br^-$, while Zn strips and plates onto the anode. ZBB is classified as a hybrid flow battery, in which one of the electrodes involves non-liquid reactants. The synergy between dissolved redox couples and metal anode usually brings great enhancement in energy density, because the volume of anolyte is eliminated.

$$\text{Cathodic: } Br_2 + 2e^- \leftrightarrow 2Br^- \ 1.09 \text{ V } vs. \text{ SHE} \quad (7)$$

$$\text{Anodic: } Zn - 2e^- \leftrightarrow Zn^{2+} \ -0.76 \text{ V } vs. \text{ SHE} \quad (8)$$

$ZnBr_2$ has high solubility over 2.0 M, but the charged species $Br_2$ is less miscible in aqueous solvent, which substantially limits the achievable energy density of the Zn-Br battery. Moreover, the stability of ZBB is challenged by the corrosivity of $Br_2$. Numerous redox couples have been studied to replace the bromine catholyte of ZBB [38–41] (Figure 2). Leung *et al.* investigated the Zn/Ce battery by employing $Zn(CH_3SO_3)_2$ and $Ce(CH_3SO_3)_3$ in $CH_3SO_3H$ electrolyte [39]. The large redox potential

between Zn and Cerium delivers a high open circuit voltage (OCV) of 2.40 V. Such a high voltage requires proper electrode materials and electrolyte additives to suppress the side reactions, which are mainly oxygen and hydrogen evolutions. Very recently, Li *et al*. reported a zinc-polyiodide battery with highly soluble $ZnI_2$ electrolyte [42]. By utilizing an ambipolar electrolyte, where both cationic and anionic ions from a single soluble compound are both energy-bearing redox active species, the electrolyte eliminated the need for non-active counter ions, such as the $Cl^-$ and $SO_4^{2-}$, commonly used in vanadium and Fe/Cr systems [43]. A high concentration $ZnI_2$ of 5.0 M was demonstrated in the reported lab cell. The energy density is claimed to be as high as 166.7 Wh· $L^{-1}$, which is comparable to lithium ion batteries. However, the high viscosity and $I_2$ precipitation have hindered the practical application of the system.

**Table 1.** A summary of simple inorganic ion redox species. SHE, standard hydrogen electrode; SCE, saturated calomel electrode.

| Redox Species | Demonstrated Concentration/mol· $L^{-1}$ | Redox Potential/V | Reference |
|---|---|---|---|
| $VCl_3/VCl_2$ | 1.0 | −0.58 *vs.* SCE | [16] |
| $Br^-/ClBr_2^-$ | 1.0 | 0.80 *vs.* SCE | [16] |
| $Cl_2/Cl^-$ | 1.0 | −1.36 *vs.* SCE | [44] |
| $Fe^{2+}/Fe^{3+}$ | 2.0 | 0.77 *vs.* SHE | [23,24] |
| $Cr^{3+}/Cr^{2+}$ | 1.0 | −0.41 *vs.* SHE | [23,24] |
| $Ti^{3+}/Ti^{4+}$ | 1.1 | 0.04 *vs.* SHE | [19] |
| $V^{3+}/V^{2+}$ | 2.0 | −0.26 *vs.* SHE (2.00 M $H_2SO_4$) | [27] |
| $VO^{2+}/VO^{2+}$ | 2.0 | 1.00 *vs.* SHE (2.00 M $H_2SO_4$) | [27] |
| $Zn/Zn^{2+}$ | | −0.76 *vs.* SHE | [27] |
| $Br_2/Br^-$ | 2.0 | 1.09 *vs.* SHE | [27] |
| $Ce^{3+}/Ce^{2+}$ | 0.5 | 1.67 *vs.* SHE | [17] |
| $Mn^{2+}/Mn^{3+}$ | 0.3 | 1.51 *vs.* SHE | [18] |
| $I^{3-}/I^-$ | 5.0 | 0.54 *vs.* SHE | [42] |
| $VBr_3/VBr_2$ | 3.0 | −0.26 *vs.* SHE | [29] |

## 3. Metal Complexes

The transition metal coordination complex comprises a transition metal center and peripheral ligands. The transition metal ion usually acts as the charge transfer center, while the potential can be tuned with different ligands. In complexes with "redox-non-innocent ligands", charges can also be stored in ligands in addition to the metal center [45]. Compared to transition metal ions, metal complexes own a considerably larger size than single metals ions, and the crossover problem can be mitigated. With the proper choice of ligand, the redox potential of the complex can be tuned towards the positive or negative direction to meet the requirements of catholyte and anolyte. Moreover, ligands can also help to improve the characteristics, such as solubility, kinetic rates and stability.

The research of metal complexes for RFB can be dated back to the 1980s [10,46–48]. Metal complexes of iron, cobalt, vanadium, cerium, chromium and ruthenium with various ligands, such as ethylenediaminetetraacetate (EDTA) [25,47], phenanthroline [10,47], triethanolamine [49] and diethylenetriaminepentaacetic acid (DTPA) [48,50], have been applied in both aqueous and non-aqueous systems. In 1988, Matsuda reported a rechargeable redox battery using tris(2,2′-bipyridine)ruthenium(II) ($[Ru(bpy)_3]^{2+}$) tetrafluoroborate in a non-aqueous electrolyte [46]. The redox couples $[Ru(bpy)_3]^{2+}/[Ru(bpy)_3]^{3+}$ and $[Ru(bpy)_3]^{+}/[Ru(bpy)_3]^{2+}$ lead to a cell voltage of about 2.60 V. A concentration of 0.20 M was demonstrated in a functional flow cell with $Et_4NClO_4/CH_3CH$ as the supporting electrolyte. Later, Chakrabarti *et al*. reported a ruthenium acetylacetonate ($Ru(acac)_3$) flow battery in tetraethyl ammonium tetrafluoroborate ($TEABF_4$)/$CH_3CN$ electrolyte. More recently, tris(2,2′-bipyridine)iron, tris(2,2′-bipyridine)nickel [51], vanadium acetylacetonate ($V(acac)_3$) [52], chromium acetylacetonate ($Cr(acac)_3$) [53–55] and

manganese acetylacetonate ($Mn(acac)_3$) [55] were studied. Among these complexes, $V(acac)_3$ attracted the most attention due to its good reversibility and a voltage of 2.20 V–2.60 V in various solvents [56]. $V(acac)_3$ shows two different voltammetry peaks, corresponding to the reactions:

$$\text{Cathodic: } V\,(acac)_3 - e^- \leftrightarrow\ [V\,(acac)_3]^+\ 0.45\ \text{V}\ vs.\ \text{Ag/Ag}^+ \tag{9}$$

$$\text{Anodic: } V\,(acac)_3 + e^- \leftrightarrow\ [V\,(acac)_3]^-\ -1.76\ \text{V}\ vs.\ \text{Ag/Ag}^+ \tag{10}$$

The reversibility has been studied on various electrode materials, on which fast electron transfer is found in the $V(acac)_3/[V(acac)_3]^+$ reaction, while a slower rate in the reduction [57]. Shinkle *et al.* studied its solubility in various solvents and supporting electrolyte, finding that the solubility were 0.59 M, 0.54 M, 0.53 M and 0.50 M in $CH_3CN$, dimethylformamide (DMF), tetrahydrofuran (THF) and dimethyl carbonate (DMC), respectively [58]. On the other hand, Herr *et al.* reported that the solubility of $V(acac)_3$ could be 0.80 M, 0.40 M, 0.25 M and 0.30 M in 1,3-dioxolane, THF, dimethyl sulfoxide (DMSO) and acetylacetone, respectively [56]. However, in the reported works, only a maximally 0.05 M concentration of $V(acac)_3$ was demonstrated in the charge/discharge tests, making the energy density far too low for real applications. Meanwhile, $V(acac)_3$ was reported to be sensitive to moisture and oxygen [59]. Further studies are required to enhance the solubility and stability of $V(acac)_3$ before it can be applied in large-scale energy storage systems.

Metallocenes, with a transition metal center sandwiched by two cyclopentadienyl groups, are usually stable and robust [60]. Hwang *et al.* reported a flow battery with ferrocene derivatives in the catholyte and cobaltocene derivatives in the anolyte. With bromoferrocene in the catholyte and bis(pentamethylcyclopentadienyl)cobalt in the anolyte, a discharge voltage of 2.20 V could be achieved [61]. In particular, ferrocene has been used as quasi-reference and overcharge protection shuttles due to its good stability and high electrochemical reaction rates [62–64]. With a redox potential of 3.20–3.60 V *vs.* $Li/Li^+$ in different organic solvents, ferrocene is also a good choice for the catholyte in a redox flow battery. Zhao *et al.* reported a ferrocene/ferrocenium redox couple as the liquid cathode [65]. $Fc/Fc^+$ showed a redox potential of 3.60 V *vs.* $Li/Li^+$ in DMF solvent, and the solubility was 0.10 M. The solubility of pristine ferrocene is still far too low to be considered as an energy storage species in a redox flow battery.

To solve this problem, Wei *et al.* reported a molecular engineering strategy of modifying the cyclopentadienyl group by adding a tetraalkylammonium pendant arm with a (trifluoromethanesulfonyl)imide ($TFSI^-$) counter anion [66]. Such a modification dramatically increased the solubility of ferrocene by 20 times in carbonate electrolyte. The modified ferrocene, which was ferrocenylmethyl dimethyl ethyl ammonium bis(trifluoromethanesulfonyl)imide (Fc1N112-TFSI), had a solubility of 1.70 M in ethylene carbonate (EC)/propylene carbonate (PC)/ethyl methyl carbonate (EMC) and 0.85 M when 1.20 M LiTFSI was added. The tetraalkylammonium group provides a positively-charged moiety, which will be the preferential sites for the carbonate molecules to be around due to the presence of polarizable oxygen atoms in carbonates that are slightly negatively charged. As a result, the interaction between solvent molecules and modified ferrocene is more favorable than pristine ferrocene. The substituent group also shifted the redox potential by +0.23 V. Thanks to the increased solubility and redox potential, a volumetric energy density of about 50 $Wh \cdot L^{-1}$ was achieved. However, the high concentration catholyte delivered lower voltage efficiency, probably because of the higher viscosity of the solution. The higher concentration also had lower Coulombic efficiency due to the more severe self-discharge.

Cappillino *et al.* reported a metal complex, tris(mnt)vanadium, (mnt = $(NC)_2C_2S_2{}^{2-}$)), with redox non-innocent ligands. Charges were stored in ligands in addition to the metal center, and as a result, redox non-innocent ligands could also contribute in the charge storage and transfer. This work presented a strong dependence of the redox potential of tris(mnt)vanadium on the cations used

in the supporting electrolyte. This unique feature may provide a convenient method to tune the redox potential by varying the supporting electrolyte.

## 4. Metal-Free Organic Compounds

Metal-centered complexes are potentially limited by the scarcity of metal elements. The toxicity of some metals, such as vanadium and chromium, also raises concerns. Metal-free compounds do not require any redox-active metals, representing a promising direction for reducing cost. [67]. Metal-free organic compounds also capitalize on the advantages of natural abundance, structural diversity, potential and solubility tunability and eco-friendliness.

Quinones are especially attractive for redox flow battery applications due to their reversible and fast proton-coupled electron transfer processes. Quinones have been used as solid active electrode materials and overcharge protection mediators in batteries [68–70]. Although good electrochemical properties of quinones have been known for many years, limited studies were carried out to employ such molecules in redox flow batteries until recent years. Among different quinones with various mother rings, benzoquinones have the highest solubility and potential [71]. In 2009, Xu and Wen reported a battery with 4,5-dihydroxy-1,3 benzenedisulfonate (DHBDS) and 2,5-dihydroxybenzenedisulfonate acid (sulfonic quinol) as the catholyte [72]. These molecules have good reversibility and relatively high potential, which are critical properties for battery applications. Although only a 0.05 M concentration was demonstrated in a lab flow battery, it showed high Coulombic efficiency of 99% in over 100 cycles, indicating that quinones are promising catholyte materials.

In early 2014, Huskinson *et al.* reported a metal-free flow battery based on 9,10-anthraquinone-2,7-disulphonic acid (AQDS) [73]. AQDS gave high solubility in aqueous solvents (over 1.0 M), and its two-electron two-proton reduction/oxidation process could theoretically double the capacity. This molecule presents a redox potential of 0.23 V *vs.* SHE (with 1.0 M $H_2SO_4$). When coupled with bromine catholyte, the flow battery could deliver a cell voltage of 0.86 V and an energy density of about 50 Wh· $L^{-1}$.

$$\text{Cathodic: } Br_2 + 2e^- \leftrightarrow 2Br^- \text{ 1.09 V } vs. \text{ SHE} \tag{11}$$

$$\text{Anodic: } 2AQDS^- + 2H^+ + 2e^- \leftrightarrow 2AQDSH \text{ 0.23 V } vs. \text{ SHE} \tag{12}$$

Yang *et al*. reported an organic redox flow battery with quinone derivatives in both the cathodic and anodic sides [74]. 1,2-benzoquinone-3,5-disulfonic acid (BQDS) was used in the catholyte, while AQDS or anthraquinone-2-sulfonic acid (AQS) was used in the anolyte. BQDS has a redox potential at 0.45 V *vs.* mercury-mercurous sulfate electrode (MSE), while the AQS and AQDS show −0.52 and −0.60 V *vs.* MSE, respectively, delivering a cell voltage of about 1.00 V. The researchers reported 1.70 M solubility of these molecules in water, although only 0.20 M was demonstrated in flow cells. More recently, Lin *et al*. reported an aqueous redox flow battery with 2,6-dihydroxyanthraquinone (2,6-DHAQ) as the anodic redox species. For the cathodic part, the bromine was replaced by $K_4Fe(CN)_6$ [75]. The cell was demonstrated with 0.5 M 2,6-DHAQ and 0.4 M $K_4Fe(CN)_6$ and showed an OCV of 1.2 V at 50% state of charge SOC. The use of quinones and ferrocyanide in catholyte provides great advantages over bromine, because they are noncorrosive and less volatile.

The attempt of applying quinone-based molecules in non-aqueous systems is hindered by the poor solubility (less than 0.05 M) of quinone in most non-aqueous electrolytes. In order to solve this problem, Wang and Xu modified the structure of anthraquinone to improve its solubility in non-aqueous electrolyte [76]. Two triethylene glycol monomethyl ether groups were added into the anthraquinone molecular structure, and the solubility was largely improved (0.25 M in $LiPF_6$/PC). Unlike the aforementioned quinone-based molecules, in which the two-electron process takes place at the same potential in aqueous electrolyte, this modified anthraquinone presented two well-separated cyclic voltammetry (CV) peaks (2.03 V and 2.27 V *vs.* $Li/Li^+$ for the reduction, and 2.47 V and

2.79 V *vs.* $Li/Li^+$ for the oxidation) in carbonate solvent. Such a big difference between the oxidative and reductive peaks (about 0.5 V) also indicated the high polarization of this molecule during charge and discharge processes.

Other than quinones, Brushett *et al*. reported an all-organic non-aqueous flow battery based on aromatic molecules [77]. 2,5-Di-*tert*-butyl-1,4-bis(2-methoxyethoxy) benzene (DBBB) was employed in the catholyte. For the anolyte side, quinoxaline-derivative 2,3,6-trimethylquinoxaline (TMeQ) was used [78]. The cell delivered a discharge voltage at 1.30–1.70 V. It is worth pointing out that only a 0.05 M concentration (for both molecules) was used in the cell test, despite much higher solubility being reported for both molecules. Later Huang *et al*. reported a liquid form molecule based on the modification of DBBB by incorporation of polyethylene oxide (PEO) chains with the dimethoxy-di-*tert*-butyl-benzene-based redox structure [79]. The new molecules present reversible redox reactions at around 4.00 V *vs.* $Li/Li^+$. In a more recent work, a new redox molecule 3,7-bis(trifluoromethyl)-*N*-ethylphenothiazine (BCF3EPT) was studied as the catholyte species [80]. The radical cation of BCF3EPT showed better stability than the radical cation of DBBB. More importantly, BCF3EPT had higher solubility in PC (1.20 M) than that of DBBB (0.20 M), and a battery consisting of 0.35 M catholyte was successfully demonstrated. On the other hand, Wei *et al*. reported 9-fluorenone and 2,5-di-*tert*-butyl-1-methoxy-4-[2′-methoxyethoxy]benzene (DBMMB) as the anolyte and catholyte redox species [81]. The solubility limit for both 9-fluorenone and DBMMB was 0.90 M in TEA-TFSI/$CH_3CN$, while 0.50 M was demonstrated in the battery test. With a redox potential of −1.64 V *vs.* $Ag/Ag^+$ for FL and 0.73 V *vs.* $Ag/Ag^+$ for DBMMB, this system delivered a voltage of 2.37 V. For these redox species, both the anolyte and catholyte reactions involve free radicals, so the selection of electrolyte is critical for the stability of radical ions.

2,2,6,6-tetramethyl-1-piperidinyloxy (TEMPO) owns quasi-reversible oxidation/reduction electrochemical properties. The TEMPO radical is protected by the resonance structures over the radical center and the alicyclic-nitroxyl structures around the center, which makes it robust in batteries for a sufficiently long time [82]. Previously, TEMPO and TEMPO-based polyradicals have been studied as cathode active materials in rechargeable batteries [83]. TEMPO has also been studied as a charge catalyst for a Li-$O_2$ battery and a Mg-$O_2$ battery [82,84–87]. In 2014, Wei *et al*. reported a high concentration TEMPO solution in EC/PC/EMC solvent [88]. The solubility of TEMPO can be as high as 5.2 M. Even with $LiPF_6$ as the supporting electrolyte, the solubility of TEMPO can still achieve 2.0 M. This high solubility might be attributed to the similar polarity between TEMPO and the carbonate solvents. In Wei's study, the TEMPO solution was coupled with a lithium-graphite anode, forming a hybrid flow battery. Due to the high concentration (2.0 M) and high potential (3.50 V *vs.* Li/Li), the flow cell delivered an energy density of 126 $Wh \cdot L^{-1}$, about five-times that of the aqueous all-vanadium flow battery. However, the high concentration causes relatively high viscosity. On the other hand, ionic liquid is an attractive approach to achieve high energy density, because it maximized the solubility of active species. Takechi *et al*. reported TEMPO-based ionic liquid as the catholyte for a redox flow battery [89]. Instead of non-substituted TEMPO molecules, this study selected 4-methoxy-2,2,6,6-tetra-methylpiperidine 1-oxyl (MT or MeO-TEMPO) as a redox compound. When MeO-TEMPO was mixed with lithium bis(trifluoromethanesulfonyl) imide (LITFSI), the mixture exhibited a self-melting behavior and formed a "smooth viscous liquid". This liquid was stable over a wide temperature range. The MeO-TEMPO/LITFSI (1/1) + $H_2O$ (17 wt %) was recognized as having well-balanced energy density and viscosity, which had over a 2.0 M concentration and a 72 mPa·s viscosity. A summary of metal complexes and metal-free organic compounds is shown in Table 2.

**Table 2.** Summary of metal complexes and metal-free organic compounds. acac, acetylacetonate; Fc1N112-TFSI, ferrocenylmethyl dimethyl ethyl ammonium bis(trifluoromethanesulfonyl)imide; DME, 1,2-dimethoxyethane.

| Redox Species | Demonstrated Concentration/M | Potential/V | Electrolyte | Reference |
|---|---|---|---|---|
| **$[Fe(bpy)_3]^{2+}/[Fe(bpy)_3]^{3+}$**<br>**$[Fe(bpy)_3]^{+}/[Fe(bpy)_3]^{2+}$** | 0.40<br>0.20 | 1.45 *vs.* $Ag/Ag^+$<br>−1.12 *vs.* $Ag/Ag^+$ | 0.5 mol· $L^{-1}$ $TEABF_4/PC$ | [46] |
| **$V(acac)_3/[V(acac)_3]^+$**<br>**$V(acac)_3/[V(acac)_3]^-$** | 0.05<br>0.05 | 0.45 *vs.* $Ag/Ag^+$<br>−1.75 *vs.* $Ag/Ag^+$ | $TBAPF_4$ in various solvents | [52,56–59] |
| **$Cr(acac)_3/[Cr(acac)_3]^+$**<br>**$Cr(acac)_3/[Cr(acac)_3]^-$** | 0.05<br>0.05 | 1.20 *vs.* $Ag/Ag^+$<br>−2.20 *vs.* $Ag/Ag^+$ | 0.5 mol· $L^{-1}$ $TEABF_4/CH_3CN$ | [54] |
| **$Mn(acac)_3/[Mn(acac)_3]^+$**<br>**$Mn(acac)_3/[Mn(acac)_3]^-$** | 0.05<br>0.05 | 0.70 *vs.* $Ag/Ag^+$<br>−0.40 *vs.* $Ag/Ag^+$ | 0.5 mol· $L^{-1}$ $TEABF_4/CH_3CN$ | [55] |
| **$Ru(acac)_3/[Ru(acac)_3]^+$**<br>**$Ru(acac)_3/[Ru(acac)_3]^+$** | 0.002<br>0.002 | 1.17 *vs.* $Ag/Ag^+$<br>−0.60 *vs.* $Ag/Ag^+$ | 1 mol· $L^{-1}$ $TEABF_4/CH_3CN$ | [53] |
| **$[Fe(bpy)_3]^{2+}/[Fe(bpy)_3]^{3+}$**<br>**$[Fe(bpy)_3]^{+}/[Fe(bpy)_3]^{2+}$** | 0.40<br>0.40 | 0.50 *vs.* $Ag/Ag^+$<br>−1.95 *vs.* $Ag/Ag^+$ | 0.5 mol· $L^{-1}$ Tetrabutylammonium hexafluorophosphate ($TEAPF_6$)/$CH_3CN$ | [53] |
| **$[Ni(bpy)_3]^{2+}/[Ni(bpy)_3]^{3+}$**<br>**$Fc/Fc^+$** | 0.20<br>0.10 | −1.70 *vs.* $Ag/Ag^+$<br>3.20–3.60 *vs.* $Li/Li^+$ | 0.5 mol· $L^{-1}$ $TEABF_4/PC$<br>Various electrolytes | [97]<br>[61,65] |
| **$CoCp_2/CoCp_2^+$**<br>**$FcBr/FcBr^+$**<br>**Bis(pentamethylcyclopentadienyl)cobalt ($CoCp^*_2/CoCp^*_2{}^+$)** | 0.01<br>0.01<br>0.01 | −1.29 *vs.* $Ag/Ag^+$<br>0.26 *vs.* $Ag/Ag^+$<br>−1.83 *vs.* $Ag/Ag^+$ | 1 mol· $L^{-1}$ $TEAPF_6/CH_3CN$ | [61] |
| **Auinoxaline-derivative 2,3,6-trimethylquinoxaline (TMeQ/$TMeQ^+$)** | 0.05 | 2.30 *vs.* $Li/Li^+$ | 0.2 mol· $L^{-1}$ $LiBF_4/PC$ | [77] |
| **3,7-bis(trifluoromethyl)-*N*-ethylphenothiazine ($BCF_3EPT/BCF_3EPT$)** | 0.35 | 3.90 and 4.40 *vs.* $Li/Li^+$ | 0.2 mol· $L^{-1}$ $LiBF_4/PC$ | [80] |
| **Fc1N112-TFSI** | 0.80 | 3.49 *vs.* $Li/Li^+$ | 1 mol· $L^{-1}$ LiTFSI in EC/PC/EMC | [66] |
| **2,2,6,6-Tetramethylpiperidine-1-oxyl (TEMPO)** | 2.00 | 3.50 *vs.* $Li/Li^+$ | 2.3 mol· $L^{-1}$ $LiPF_6$ in EC/PC/EMC | [88] |
| **4-Methoxy-2,2,6,6-tetra-methylpiperidine1-oxyl (Meo-TEMPO)** | MeO-TEMPO/LITFSI (1/1) + $H_2O$(17% wt) | 3.50 *vs.* $Li/Li^+$ | Ionic liquid | [89] |
| **9-fluorenone** | 0.50 | −1.64 *vs.* $Ag/Ag^+$ | Various lithium salts in DME or $CH_3CN$ [81] | [81] |
| **2,5-di-*tert*-Butyl-1-methoxy-4-[2′-methoxyethoxy]benzene (DBMMB)** | 0.50 | 0.73 *vs.* $Ag/Ag^+$ | | |
| **2,5-di-*tert*-Butyl-1,4-bis(2-methoxyethoxy)benzene ($DBBB/DBBB^+$)** | 0.05 | 4.00 *vs.* $Li/Li^+$ | 0.2 mol· $L^{-1}$ $LiBF_4/PC$ | [77] |
| **$V(mnt)_3{}^{2-}/V(mnt)_3{}^-$**<br>**$V(mnt)_3{}^-/V(mnt)_3$** | 0.02<br>0.02 | −1.41 to −1.25 *vs.* SHE;<br>−0.23 *vs.* SHE | Various $PF_6{}^-$ salts in $CH_3CN$ | [45] |
| **2,6-dihydroxyanthraquinone (2,6-DHAQ)**<br>**$K_4Fe(CN)_6$** | 0.50<br>0.4 | −0.70 *vs.* SHE<br>0.50 *vs.* SHE | 1.0 M $KOH/H_2O$ | [75] |

* stands for the deca-methyl groups in the Bis(pentamethylcyclopentadienyl)cobalt structure.

## 5. Polysulfide/Sulfur

Sulfur has drawn considerable attention for its high theoretical capacity, non-toxicity and low cost [90]. The aqueous polysulfide/bromine battery (PSB) utilizes $Na_2S$ in the anolyte, coupled with NaBr as the catholyte [91]. $Na_2S$ is both abundant and cost-effective, and it gives high solubility in aqueous solvents. A 2.0 M $Na_2S$ electrolyte has been demonstrated in redox flow batteries [92,93]. A cell voltage of about 1.36 V is given by such a system. Long chain polysulfides also show good solubility in non-aqueous electrolytes [94]. Yang *et al*. reported a membrane-free Li/polysulfide hybrid flow battery with 1,3-dioxolane (DOL)/1,2-dimethoxyethane (DME) as the solvent [95]. Polysulfide had an ultra-high theoretical solubility of 7.0 M in such an electrolyte. To avoid the formation of solid $Li_2S_2$ and $Li_2S$ phases, the catholyte was cycled between sulfur and $Li_2S_4$. The proof-of-concept Li/polysulfide battery demonstrated a 5.0 M $Li_2S_8$ catholyte, giving a theoretical energy density of 95 Wh$\cdot$ kg$^{-1}$ and 106 Wh$\cdot$ L$^{-1}$. It is worth noting that the cycling test was conducted in a coin cell without flowing, although the researchers claimed that the chemistry could be applied in flow conditions. Despite the high solubility of polysulfide, solid precipitation due to the insoluble short-chain polysulfides formed during long-term cell cycling still remains a problem [96]. Pan *et al*. investigated the solution chemistry of polysulfides in organic electrolyte [94]. The solubility of short chain polysulfides, like $Li_2S_2$, can be slightly improved by using DMSO/LiTf as the supporting electrolyte.

## 6. Li Metal

Lithium is known to have the highest theoretical specific capacity of 3860 mAh/g and a molar lithium concentration of 76.95 M. Meanwhile, as an anodic electrode, lithium provides lower potential (−3.04 V *vs.* standard hydrogen electrode (SHE)) than most redox species, and it is advantageous to obtain a high cell voltage [98]. Therefore, synergy with Li metal seems to be an attractive way to improve the energy density of redox flow battery systems. In 2011, a lithium hybrid flow battery with a lithium metal anode and an aqueous flow catholyte was reported by Goodenough's group [99,100]. In the demonstrated battery, 0.1 M $K_3Fe(CN)_6$ solution was used as the catholyte. Despite the moderate concentration of catholyte, the hybrid flow battery presented a high cell voltage of 3.40 V, which was much higher than conventional aqueous flow batteries. A similar system was also proposed by Zhou and coworkers, and $Fe^{3+}/Fe^{2+}$ was employed as the cathodic redox couple. The electrode reactions of hybrid flow batteries can be described as follows:

$$\text{Cathodic: } M^+ + e^- \leftrightarrow M \tag{13}$$

$$\text{Anodic: } Li - e^- \leftrightarrow Li^+ \tag{14}$$

As shown in Figure 3, the basic setup of a lithium metal hybrid flow battery consists of an anodic compartment with lithium metal in organic electrolyte, a flow through cathode and a solid electrolyte membrane. By combining lithium metal with circulating catholyte, the hybrid flow battery incorporates the advantages of a higher energy density from the lithium battery and independent operation of the power generation and energy storage from the redox flow battery [15].

The key component of the lithium hybrid redox flow battery is the solid electrolyte membrane. In addition to a high $Li^+$ conductivity, the membrane is required to block the dendrite growth and redox species crossover. Moreover, the membrane must be mechanically and chemically stable in the cell operation. Currently, the development of a solid electrolyte membrane is still far from being mature. The commercially-available solid electrolyte membranes, including LATP (like $Li_{1.4}Al_{0.4}Ti_{1.6}(PO_4)_3$) and LAGP (like $Li_{1.5}Al_{0.5}Ge_{1.5}(PO_4)_3$), are generally expensive. Under this circumstance, some reports employ a "membrane-free" configuration in non-aqueous systems with a solid electrolyte interface (SEI) layer to protect the lithium metal anode [66,101,102]. Ding *et al*. demonstrated a membrane-free lithium hybrid flow battery with ferrocene/ferrocenium in the catholyte [102]. Due to the fast rate

constant of $Fc/Fc^+$ and low internal resistance, peak power output reached 4700 $W \cdot L^{-1}$. While the long-term cycling performance is unlikely to be solved, the membrane-free configuration eliminates the need for a solid electrolyte membrane, considerably reducing the cost and allowing for higher power density.

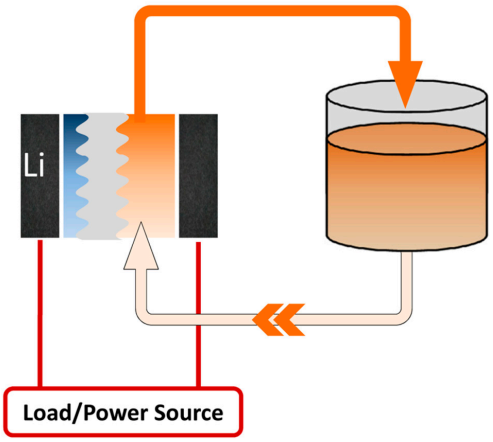


**Figure 3.** Illustration of a lithium hybrid flow battery. The anodic side consists of lithium metal and organic electrolyte, while the catholyte is circulated.

Since the anodic potential and capacity have been fixed by lithium metal, the selection of the catholyte is critical for the overall performance of a lithium hybrid flow battery. High solubility and high redox potential are desirable for catholyte redox species. The reported catholytes have covered various redox couples, ranging from an aqueous system to a non-aqueous system, including transition metal ions, halogen ions [103–106], metal complexes [65], sulfur/polysulfide, metal-free species, *etc.* Compared to traditional RFBs, the hybrid flow battery with lithium metal anode possesses advantages of a higher operating voltage, a smaller volume and a simple design. Especially, the energy density of the redox flow battery increases drastically by the introduction of a lithium metal anode. However, it should be pointed out that the hybrid configuration loses the flexibility in the anodic compartment, since the lithium metal anode is in static mode rather than flow mode. In addition, the lithium metal anode has problems of poor cycling performance, deleterious dendrite growth and safety concerns.

## 7. Semi-Solid Flow Battery

Duduta *et al.* proposed a semi-solid approach, in which Li-intercalation active materials are circulated in slurries with conductive additives [107]. The main reactions in semi-solid slurries are $Li^+$ intercalation and extraction, which is fundamentally different from the abovementioned electrolytes. By employing the active material suspensions rather than the solution, the energy density is no longer limited by the solubility of active species. Solid storage compounds generally contain lithium with a high concentration. For example, the theoretical molar concentration of lithium is about 51.6 M in $LiCoO_2$. Although usually only half of the $Li^+$ in $LiCoO_2$ is usable, the concentration is still considerably high. With the high concentration of solid materials and the wide potential range of non-aqueous solvent, the semi-solid flow battery could be able to deliver high energy density, while keeping the flexibility of the flow battery and avoiding lithium dendrite growth. In Duduta's report, a semi-solid flow battery that employed $LiCoO_2$ (20 vol %, 10.2 M and 1.5% Ketjenblack) as the cathode and $Li_4Ti_5O_{12}$ (10 vol %, 2.3 M and 2% Ketjenblack) as the anode was demonstrated.

Later, Hamelet *et al.* applied the semi-solid concept to a silicon suspension flow battery [108]. Silicon is attractive as an anodic active material for its high lithium retention ability, but the large volume change has hindered its development. The semi-solid configuration seems to be suitable to

employ silicon, since the volume change will be less problematic in the suspension. Fan *et al*. reported a polysulfide flow battery with a percolating nanoscale conductor network [109]. The polysulfide species are converted reversibly between $Li_2S_8$ and $Li_2S$. More recently, Chen *et al*. employed a sulfur-impregnated flow cathode with 20 vol % sulfur and 26 vol % carbon [110]. The volumetric capacity resulting from such a concentration was 12.9 M, leading to a high volumetric capacity, despite the demonstration cell being tested under a very small scale by a syringe pump with 100 μL of electrolyte. Edgar Ventosa *et al*. proposed a non-aqueous semi-solid flow battery based on $Na^+$ chemistry using $Na_xNi_{0.22}Co_{0.11}Mn_{0.66}O_2$ and $NaTi_2(PO_4)_3$ as the positive and negative electrodes, respectively [111]. The semi-solid flow battery has also been applied in an aqueous system with $LiTi(PO_4)_3$ and $LiFePO_4$ as the active materials [112]. Very recently, Janoschka *et al*. reported an aqueous flow battery with micro-molecular polymers as the redox species [113]. By using a dialysis membrane, the redox-active polymers, which have a hydrodynamic radius of around 2 nm, could be effectively charged/discharged in the flow battery.

The semi-solid flow battery provides a promising approach towards higher energy density, while keeping the configuration of decoupled energy and power. However, since the active materials are mostly not electronic conductive, carbon materials need to be dispersed into the slurry to facilitate electron transfer and, thus, inevitably compromise the energy density. Moreover, the electronic conductivity of the suspension network is about 100-times lower than the ionic conductivity and is expected to be the rate-limiting step [107]. Another major concern is the high viscosity that ensues from the increasing solid load. Although this problem can be alleviated by tailoring the interaction between suspension particles, the active materials' fraction is still limited within around 20 vol % in most reports [114]. The increase in the solid fraction also results in the decrease of ionic conductivity [107]. Given these limitations, the high energy density of the solid active materials may not be fully realized in the semi-solid configuration.

## 8. Redox Flow Lithium Ion Battery

The redox targeting concept, which was first proposed by Wang *et al*. in 2006, allows the solid active materials to be charged/discharged without any conductive additives [115] (Figure 4). In 2013, Huang *et al*. reported a redox flow lithium battery (RFLB) based on redox targeting [116]. Unlike the semi-solid configuration, RFLB holds the solid material statically in the tank, and the redox shuttle molecules are circulated in the flow system (Figure 5). The electron transfer between the solid materials and current collector was conducted via the circulation of shuttle molecules. In Huang's work, ferrocene (Fc) and dibromoferrocene ($FcBr_2$) were selected as the reduction and oxidation agents. $LiFePO_4$ typically shows a potential of 3.45 V *vs.* $Li/Li^+$, while Fc is at 3.25 V and $FcBr_2$ is at 3.65 V. As a result, the charge and discharge processes could be achieved by the redox targeting reactions between $LiFePO_4$ and shuttle molecules.

Charging process:

$$FcBr_2 \rightarrow FcBr_2{}^+ + e^- \ \text{(on electrode)} \quad (15)$$

$$FcBr_2{}^+ + LiFePO_4 \rightarrow FcBr_2 + FePO_4 + Li^+ \ \text{(in tank)} \quad (16)$$

Discharging process:

$$Fc^+ + e^- \rightarrow Fc \ \text{(on electrode)} \quad (17)$$

$$Fc + \ FePO_4 + Li^+ \rightarrow Fc^+ + LiFePO_4 \quad (18)$$

On the other hand, Pan *et al*. studied the redox targeting for the anodic side of RFLB [117]. Anatase $TiO_2$ (1.80 V *vs.* $Li/Li^+$), cobaltocene (1.95 V *vs.* $Li/Li^+$) and bis(pentamethylcyclopentadienyl)cobalt (1.36 V *vs.* $Li/Li^+$) were selected as the solid materials and shuttle molecules.

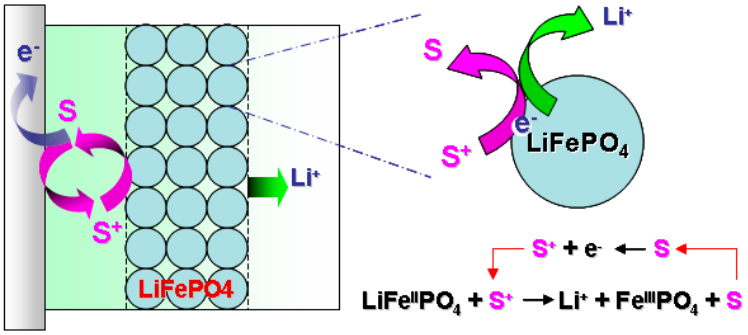


**Figure 4.** The principle of redox targeting of an insulating electrode material, such as $LiFePO_4$, by a freely-diffusing molecular shuttle, S [115] (reprinted with permission from *Angew Chem Int Ed Engl* 45, 8197–8200, (2006); Copyright 2006, WILEY-VCH Verlag GmbH & Co. KGaA, Weinheim).

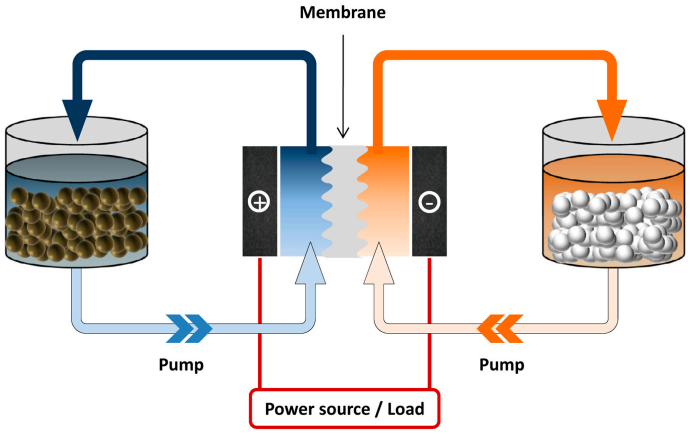


**Figure 5.** Illustration of a redox flow lithium ion battery. Solid active materials are stored statically in the tanks, while redox molecules are circulated with electrolyte fluids.

Discharging process:

$$x\mathrm{Li}^+ + \mathrm{TiO_2} + x\mathrm{CoCp^*{}_2} \rightarrow \mathrm{Li}_x\mathrm{TiO_2} + x\mathrm{CoCp^*{}_2}^+ \text{ (in tank)} \quad (19)$$

$$\mathrm{CoCp^*{}_2}^+ + \mathrm{e}^- \rightarrow \mathrm{CoCp^*{}_2} \text{ (on electrode)} \quad (20)$$

Charging process:

$$\mathrm{CoCp_2} \rightarrow \mathrm{CoCp_2}^+ + \mathrm{e}^- \text{ (on electrode)} \quad (21)$$

$$\mathrm{Li}_x\mathrm{TiO_2} + x\mathrm{CoCp_2}^+ \rightarrow x\mathrm{Li}^+ + \mathrm{TiO_2} + x\mathrm{CoCp_2} \text{ (in tank)} \quad (22)$$

Because the solid materials are immobile, the viscosity will not be a concern in RFLB. Additionally, no conducting additive is required in the charge/discharge process. As a result, a large fraction of the solid active materials is allowed in the storage tank. The molar concentration of lithium in $LiFePO_4$ is 22.0 M, while the concentration in $Li_{0.5}TiO_2$ is 22.5 M. If considering a porosity of 50% in the solid materials, the effective concentration could be above 11.0 M. Meanwhile, since most of the energy is stored in the solid materials in the tank, only a diluted concentration of shuttle molecules is needed to conduct the electrons, such as 20.0 mM reported in Huang's work and 5.0 mM in Pan's work. A low molecule concentration is meaningful to reduce the crossover contamination and to extend battery life. When $TiO_2$ and $LiFePO_4$ are combined in the full cell of RFLB, we can expect a cell voltage of about 1.65 V.

## 9. Conclusions and Perspective

Enhancing energy density is one of the most pressing issues in the development of redox flow batteries. As reviewed, recent research on RFB has proposed a variety of approaches towards higher energy density. Particularly, novel redox species have been explored to improve the concentration and cell voltage for both aqueous and non-aqueous systems. Meanwhile, integrating lithium storage materials with redox flow battery is a promising approach to unprecedentedly improve the energy density of RFB. However, some critical challenges still remain before a viable redox flow system is developed.

Although numerous redox species are proposed in non-aqueous electrolytes, most of them are focused on the catholyte, and the anodic species are fairly limited. As a result, the anolyte generally limits the energy density of the whole system. Meanwhile, the redox potential of the anolyte should be pushed lower to maximize the cell voltage. To fabricate a non-aqueous RFB with high energy density, the development of anodic species is urgently needed.

While a hybrid flow battery with a Li metal anode substantially enhances the overall energy density, the flexibility is unfortunately sacrificed in the anode. In addition, the poor cycling stability of the lithium metal anode could be a critical problem of the lithium hybrid flow battery. The cycling stability of lithium metal is deteriorated by dendritic morphology formation during lithium deposition, as well as side reactions between lithium and the electrolyte, which result in low Coulombic efficiency during repeated charging and discharging. The dendrite growth on the metal anode also raises great safety concerns. To address these problems, an anolyte with low potential and high capacity is required to replace the metal anode.

Filling the storage tanks with solid/semi-solid active materials is an effective way to increase the energy density. The redox-targeting concept provides an elegant way for the electron transfer between active materials and current collectors. With the assistance of redox shuttle molecules, the solid active materials could be reversibly charged/discharged while remaining static in tanks. This concept is very promising towards higher energy density. To increase cell voltage, higher potential solid materials, like $LiCoO_2$, $LiMnPO_4$ and $LiVPO_4F$, should be employed in the cathodic side; and accordingly, lower potential solid materials, like $Li_4Ti_5O_{12}$, will be suitable for the anodic side. To reduce the overpotential loss, redox molecules matching the potentials of solid materials should also be explored.

**Acknowledgments:** We acknowledge financial support by the National Research Foundation, Prime Minister's Office, Singapore, under its Competitive Research Program (CRP Award No. NRF-CRP8-2011-04).

**Author Contribution:** Feng Pan conducted the literature review and drafted the manuscript. Qing Wang supervised the writing, revised and approved the final manuscript.

**Conflicts of Interest:** The authors declare no conflict of interest.

## References

1. Lewis, N.S. Powering the planet. *MRS Bull.* **2007**, *32*, 808–820. [CrossRef]
2. Echeverría, D.; Gass, P. *The United States and China's New Climate Change Commitments: Elements, Implications and Reactions*; The International Institute for Sustainable Development: Winnipeg, MB, Canada, 2014.
3. Larcher, D.; Tarascon, J.M. Towards greener and more sustainable batteries for electrical energy storage. *Nat. Chem.* **2015**, *7*, 19–29. [CrossRef] [PubMed]
4. Skyllas-Kazacos, M.; Chakrabarti, M.H.; Hajimolana, S.A.; Mjalli, F.S.; Saleem, M. Progress in Flow Battery Research and Development. *J. Electrochem. Soc.* **2011**, *158*, R55–R79. [CrossRef]
5. Thaller, L.H. Electrically rechargeable redox flow cell. In Proceedings of the 9th Intersociety Energy Conversion Engineering Conference, San Francisco, CA, USA, 26–30 August 1976.
6. Weber, A.Z.; Mench, M.M.; Meyers, J.P.; Ross, P.N.; Gostick, J.T.; Liu, Q. Redox flow batteries: A review. *J. Appl. Electrochem.* **2011**, *41*, 1137–1164. [CrossRef]
7. Alotto, P.; Guarnieri, M.; Moro, F. Redox flow batteries for the storage of renewable energy: A review. *Renew. Sustain. Energy Rev.* **2014**, *29*, 325–335. [CrossRef]

8. Chiang, Y.-M. Building a better battery. *Science* **2010**, *330*, 1485–1486. [CrossRef] [PubMed]
9. Wang, W.; Luo, Q.; Li, B.; Wei, X.; Li, L.; Yang, Z. Recent Progress in Redox Flow Battery Research and Development. *Adv. Funct. Mater.* **2013**, *23*, 970–986. [CrossRef]
10. Chen, Y.W.D.; Santhanam, K.; Bard, A.J. Solution Redox Couples for Electrochemical Energy Storage I. Iron(III)-Iron(II) Complexes with O-Phenanthroline and Related Ligands. *J. Electrochem. Soc.* **1981**, *128*, 1460–1467. [CrossRef]
11. Ponce de León, C.; Frías-Ferrer, A.; González-García, J.; Szánto, D.A.; Walsh, F.C. Redox flow cells for energy conversion. *J. Power Sources* **2006**, *160*, 716–732. [CrossRef]
12. Li, X.; Zhang, H.; Mai, Z.; Zhang, H.; Vankelecom, I. Ion exchange membranes for vanadium redox flow battery (VRB) applications. *Energy Environ. Sci.* **2011**, *4*, 1147–1160. [CrossRef]
13. Shin, S.-H.; Yun, S.-H.; Moon, S.-H. A review of current developments in non-aqueous redox flow batteries: Characterization of their membranes for design perspective. *RSC Adv.* **2013**, *3*, 9095–9116. [CrossRef]
14. Leung, P.; Li, X.; Ponce de León, C.; Berlouis, L.; Low, C.T.J.; Walsh, F.C. Progress in redox flow batteries, remaining challenges and their applications in energy storage. *RSC Adv.* **2012**, *2*, 10125–10156. [CrossRef]
15. Wang, Y.; He, P.; Zhou, H. Li-Redox Flow Batteries Based on Hybrid Electrolytes: At the Cross Road between Li-ion and Redox Flow Batteries. *Adv. Energy Mater.* **2012**, *2*, 770–779. [CrossRef]
16. Skyllas-Kazacos, M. Novel vanadium chloride/polyhalide redox flow battery. *J. Power Sources* **2003**, *124*, 299–302. [CrossRef]
17. Xia, X.; Liu, H.-T.; Liu, Y. Studies of the Feasibility of a $Ce^{4+}/Ce^{3+}$ $V^{2+}/V^{3+}$ Redox Cell. *J. Electrochem. Soc.* **2002**, *149*, A426–A430. [CrossRef]
18. Xue, F.-Q.; Wang, Y.-L.; Wang, W.-H.; Wang, X.-D. Investigation on the electrode process of the Mn(II)/Mn(III) couple in redox flow battery. *Electrochim. Acta* **2008**, *53*, 6636–6642. [CrossRef]
19. Wang, Y.; Lin, M.; Wan, C. A study of the discharge performance of the Ti/Fe redox flow system. *J. Power Sources* **1984**, *13*, 65–74. [CrossRef]
20. Sanz, L.; Lloyd, D.; Magdalena, E.; Palma, J.; Kontturi, K. Description and performance of a novel aqueous all-copper redox flow battery. *J. Power Sources* **2014**, *268*, 121–128. [CrossRef]
21. Peljo, P.; Lloyd, D.; Doan, N.; Majaneva, M.; Kontturi, K. Towards A Thermally Regenerative All-Copper Redox Flow Battery. *Phys. Chem. Chem. Phys.* **2014**, *16*, 2831–2835. [CrossRef] [PubMed]
22. Wen, Y.; Zhang, H.; Qian, P.; Zhou, H.; Zhao, P.; Yi, B.; Yang, Y. Studies on Iron ($Fe^{3+}/Fe^{2+}$)-Complex/Bromine ($Br^2/Br^-$) Redox Flow Cell in Sodium Acetate Solution. *J. Electrochem. Soc.* **2006**, *153*, A929–A934. [CrossRef]
23. Thaller, L. Redox flow cell energy storage systems. In Proceedings of the Terrestrial Energy Systems Conference, Orlando, FL, USA, 4–6 June 1979; American Institute of Aeronautics and Astronautics: New York, NY, USA, 1979.
24. Gahn, R.F.; Hagedorn, N.H.; Ling, J.S. *Single Cell Performance Studies on the Fe/Cr Redox Energy Storage System Using Mixed Reactant Solutions at Elevated Temperature*; National Aeronautics and Space Administration, Lewis Research Center: Brook Park, OH, USA, 1983.
25. Bae, C.H.; Roberts, E.P.L.; Dryfe, R.A.W. Chromium redox couples for application to redox flow batteries. *Electrochim. Acta* **2002**, *48*, 279–287. [CrossRef]
26. Skyllas-Kazacos, M.; Grossmith, F. Efficient vanadium redox flow cell. *J. Electrochem. Soc.* **1987**, *134*, 2950–2953. [CrossRef]
27. Sum, E.; Rychcik, M.; Skyllas-Kazacos, M. Investigation of the V(V)/V(IV) system for use in the positive half-cell of a redox battery. *J. Power Sources* **1985**, *16*, 85–95. [CrossRef]
28. Rydh, C.J.; Sandén, B.A. Energy analysis of batteries in photovoltaic systems. Part II: Energy return factors and overall battery efficiencies. *Energy Convers. Manag.* **2005**, *46*, 1980–2000. [CrossRef]
29. Skyllas-Kazacos, M.; Kazacos, G.; Poon, G.; Verseema, H. Recent advances with UNSW vanadium-based redox flow batteries. *Int. J. Energy Res.* **2010**, *34*, 182–189. [CrossRef]
30. Díaz-González, F.; Sumper, A.; Gomis-Bellmunt, O.; Villafáfila-Robles, R. A review of energy storage technologies for wind power applications. *Renew. Sustain. Energy Rev.* **2012**, *16*, 2154–2171. [CrossRef]
31. Dunn, B.; Kamath, H.; Tarascon, J.-M. Electrical energy storage for the grid: A battery of choices. *Science* **2011**, *334*, 928–935. [CrossRef] [PubMed]
32. Soloveichik, G.L. Battery technologies for large-scale stationary energy storage. *Annu. Rev. Chem. Biomol. Eng.* **2011**, *2*, 503–527. [CrossRef] [PubMed]

33. Tantisakon, T.; Holasut, K. Prospects of Carbon Based Micro-Fluid Electrolyte for the Vanadium Redox Flow Battery (VRB). *Adv. Mater. Res.* **2014**, *931*, 1083–1088. [CrossRef]
34. Wang, W.; Kim, S.; Chen, B.; Nie, Z.; Zhang, J.; Xia, G.-G.; Li, L.; Yang, Z. A new redox flow battery using Fe/V redox couples in chloride supporting electrolyte. *Energy Environ. Sci.* **2011**, *4*, 4068–4073. [CrossRef]
35. Hosseiny, S.S.; Saakes, M.; Wessling, M. A polyelectrolyte membrane-based vanadium/air redox flow battery. *Electrochem. Commun.* **2011**, *13*, 751–754. [CrossRef]
36. Menictas, C.; Skyllas-Kazacos, M. Performance of vanadium-oxygen redox fuel cell. *J. Appl. Electrochem.* **2011**, *41*, 1223–1232. [CrossRef]
37. Lim, H.; Lackner, A.; Knechtli, R. Zinc-bromine secondary battery. *J. Electrochem. Soc.* **1977**, *124*, 1154–1157. [CrossRef]
38. Zhang, L.; Lai, Q.; Zhang, J.; Zhang, H. A high-energy-density redox flow battery based on zinc/polyhalide chemistry. *ChemSusChem* **2012**, *5*, 867–869. [CrossRef] [PubMed]
39. Leung, P.K.; Ponce-de-León, C.; Low, C.T.J.; Shah, A.A.; Walsh, F.C. Characterization of a zinc–cerium flow battery. *J. Power Sources* **2011**, *196*, 5174–5185. [CrossRef]
40. Manjunatha, H.; Suresh, G.S.; Venkatesha, T.V. Electrode materials for aqueous rechargeable lithium batteries. *J. Solid State Electrochem.* **2011**, *15*, 431–445. [CrossRef]
41. Yang, Z.; Zhang, J.; Kintner-Meyer, M.C.; Lu, X.; Choi, D.; Lemmon, J.P.; Liu, J. Electrochemical energy storage for green grid. *Chem. Rev.* **2011**, *111*, 3577–3613. [CrossRef] [PubMed]
42. Li, B.; Nie, Z.; Vijayakumar, M.; Li, G.; Liu, J.; Sprenkle, V.; Wang, W. Ambipolar zinc-polyiodide electrolyte for a high-energy density aqueous redox flow battery. *Nature Commun.* **2015**, *6*, 6303. [CrossRef] [PubMed]
43. Kear, G.; Shah, A.A.; Walsh, F.C. Development of the all-vanadium redox flow battery for energy storage: A review of technological, financial and policy aspects. *Int. J. Energy Res.* **2012**, *36*, 1105–1120. [CrossRef]
44. Linden, D.; Reddy, T.B. *Handbook of Batteries*; McGraw-Hill Companies, Inc.: New York, NY, USA, 2002.
45. Cappillino, P.J.; Pratt, H.D.; Hudak, N.S.; Tomson, N.C.; Anderson, T.M.; Anstey, M.R. Application of Redox Non-Innocent Ligands to Non-Aqueous Flow Battery Electrolytes. *Adv. Energy Mater.* **2014**, *4*. [CrossRef]
46. Matsuda, Y.; Tanaka, K.; Okada, M.; Takasu, Y.; Morita, M.; Matsumura-Inoue, T. A rechargeable redox battery utilizing ruthenium complexes with non-aqueous organic electrolyte. *J. Appl. Electrochem.* **1988**, *18*, 909–914. [CrossRef]
47. Ibanez, J.G.; Choi, C.S.; Becker, R.S. Aqueous redox transition metal complexes for electrochemical applications as a function of pH. *J. Electrochem. Soc.* **1987**, *134*, 3083–3089. [CrossRef]
48. Murthy, A.S.N.; Srivastava, T. Fe(III)/Fe(II)—Ligand systems for use as negative half-cells in redox-flow cells. *J. Power Sources* **1989**, *27*, 119–126. [CrossRef]
49. Wen, Y.H.; Zhang, H.M.; Qian, P.; Zhou, H.T.; Zhao, P.; Yi, B.L.; Yang, Y.S. A study of the Fe(III)/Fe(II)–triethanolamine complex redox couple for redox flow battery application. *Electrochim. Acta* **2006**, *51*, 3769–3775. [CrossRef]
50. Modiba, P.; Matoetoe, M.; Crouch, A.M. Kinetics study of transition metal complexes (Ce–DTPA, Cr–DTPA and V–DTPA) for redox flow battery applications. *Electrochim. Acta* **2013**, *94*, 336–343. [CrossRef]
51. Mun, J.; Lee, M.-J.; Park, J.-W.; Oh, D.-J.; Lee, D.-Y.; Doo, S.-G. Non-Aqueous Redox Flow Batteries with Nickel and Iron Tris(2,2′-bipyridine) Complex Electrolyte. *Electrochem. Solid State Lett.* **2012**, *15*, A80–A82. [CrossRef]
52. Liu, Q.; Sleightholme, A.E.S.; Shinkle, A.A.; Li, Y.; Thompson, L.T. Non-aqueous vanadium acetylacetonate electrolyte for redox flow batteries. *Electrochem. Commun.* **2009**, *11*, 2312–2315. [CrossRef]
53. Chakrabarti, M.H.; Dryfe, R.A.W.; Roberts, E.P.L. Evaluation of electrolytes for redox flow battery applications. *Electrochim. Acta* **2007**, *52*, 2189–2195. [CrossRef]
54. Liu, Q.; Shinkle, A.A.; Li, Y.; Monroe, C.W.; Thompson, L.T.; Sleightholme, A.E.S. Non-aqueous chromium acetylacetonate electrolyte for redox flow batteries. *Electrochem. Commun.* **2010**, *12*, 1634–1637. [CrossRef]
55. Sleightholme, A.E.S.; Shinkle, A.A.; Liu, Q.; Li, Y.; Monroe, C.W.; Thompson, L.T. Non-aqueous manganese acetylacetonate electrolyte for redox flow batteries. *J. Power Sources* **2011**, *196*, 5742–5745. [CrossRef]
56. Herr, T.; Noack, J.; Fischer, P.; Tübke, J. 1,3-Dioxolane, tetrahydrofuran, acetylacetone and dimethyl sulfoxide as solvents for non-aqueous vanadium acetylacetonate redox-flow-batteries. *Electrochim. Acta* **2013**, *113*, 127–133. [CrossRef]
57. Shinkle, A.A.; Sleightholme, A.E.S.; Thompson, L.T.; Monroe, C.W. Electrode kinetics in non-aqueous vanadium acetylacetonate redox flow batteries. *J. Appl. Electrochem.* **2011**, *41*, 1191–1199. [CrossRef]

58. Shinkle, A.A.; Pomaville, T.J.; Sleightholme, A.E.S.; Thompson, L.T.; Monroe, C.W. Solvents and supporting electrolytes for vanadium acetylacetonate flow batteries. *J. Power Sources* **2014**, *248*, 1299–1305. [CrossRef]
59. Shinkle, A.A.; Sleightholme, A.E.S.; Griffith, L.D.; Thompson, L.T.; Monroe, C.W. Degradation mechanisms in the non-aqueous vanadium acetylacetonate redox flow battery. *J. Power Sources* **2012**, *206*, 490–496. [CrossRef]
60. Astruc, D. Electron-reservoir complexes and other redox-robust reagents: Functions and applications. *New J. Chem.* **2009**, *33*, 1191–1206. [CrossRef]
61. Hwang, B.; Park, M.S.; Kim, K. Ferrocene and Cobaltocene Derivatives for Non-Aqueous Redox Flow Batteries. *ChemSusChem* **2015**, *8*, 310–314. [CrossRef] [PubMed]
62. Allen, J.B.; Larry, R.F. *Electrochemical Methods: Fundamentals and Applications*; Department of Chemistry and Biochemistry University of Texas at Austin: Austin, TX, USA; John Wiley & Sons, Inc.: New York, NY, USA, 2001; pp. 156–176.
63. Ates, M.N.; Allen, C.J.; Mukerjee, S.; Abraham, K.M. Electronic Effects of Substituents on Redox Shuttles for Overcharge Protection of Li-ion Batteries. *J. Electrochem. Soc.* **2012**, *159*, A1057–A1064. [CrossRef]
64. Laoire, C.O.; Plichta, E.; Hendrickson, M.; Mukerjee, S.; Abraham, K.M. Electrochemical studies of ferrocene in a lithium ion conducting organic carbonate electrolyte. *Electrochim. Acta* **2009**, *54*, 6560–6564. [CrossRef]
65. Zhao, Y.; Ding, Y.; Song, J.; Li, G.; Dong, G.; Goodenough, J.B.; Yu, G. Sustainable Electrical Energy Storage through the Ferrocene/Ferrocenium Redox Reaction in Aprotic Electrolyte. *Angew. Chem. Int. Ed.* **2014**, *53*, 11036–11040. [CrossRef] [PubMed]
66. Wei, X.; Cosimbescu, L.; Xu, W.; Hu, J.Z.; Vijayakumar, M.; Feng, J.; Hu, M.Y.; Deng, X.; Xiao, J.; Liu, J.; *et al*. Towards High-Performance Nonaqueous Redox Flow Electrolyte via Ionic Modification of Active Species. *Adv. Energy Mater.* **2015**, *5*. [CrossRef]
67. Armand, M.; Tarascon, J.-M. Building better batteries. *Nature* **2008**, *451*, 652–657. [CrossRef] [PubMed]
68. Yao, M.; Senoh, H.; Yamazaki, S.-I.; Siroma, Z.; Sakai, T.; Yasuda, K. High-capacity organic positive-electrode material based on a benzoquinone derivative for use in rechargeable lithium batteries. *J. Power Sources* **2010**, *195*, 8336–8340. [CrossRef]
69. Zhang, L.; Zhang, Z.; Redfern, P.C.; Curtiss, L.A.; Amine, K. Molecular engineering towards safer lithium-ion batteries: A highly stable and compatible redox shuttle for overcharge protection. *Energy Environ. Sci.* **2012**, *5*, 8204–8207. [CrossRef]
70. Senoh, H.; Yao, M.; Sakaebe, H.; Yasuda, K.; Siroma, Z. A two-compartment cell for using soluble benzoquinone derivatives as active materials in lithium secondary batteries. *Electrochim. Acta* **2011**, *56*, 10145–10150. [CrossRef]
71. Biilmann, E. Oxidation and reduction potentials of organic compounds. *Trans. Faraday Soc.* **1924**, *19*, 676–691. [CrossRef]
72. Xu, Y.; Wen, Y.; Cheng, J.; Yanga, Y.; Xie, Z.; Cao, G. Novel organic redox flow batteries using soluble quinonoid compounds as positive materials. In Proceedings of the World Non-Grid-Connected Wind Power and Energy Conference, Nanjing, China, 24–26 September 2009; pp. 1–4.
73. Huskinson, B.; Marshak, M.P.; Suh, C.; Er, S.; Gerhardt, M.R.; Galvin, C.J.; Chen, X.; Aspuru-Guzik, A.; Gordon, R.G.; Aziz, M.J. A metal-free organic–inorganic aqueous flow battery. *Nature* **2014**, *505*, 195–198. [CrossRef] [PubMed]
74. Yang, B.; Hoober-Burkhardt, L.; Wang, F.; Surya Prakash, G.K.; Narayanan, S.R. An Inexpensive Aqueous Flow Battery for Large-Scale Electrical Energy Storage Based on Water-Soluble Organic Redox Couples. *J. Electrochem. Soc.* **2014**, *161*, A1371–A1380. [CrossRef]
75. Lin, K.; Chen, Q.; Gerhardt, M.R.; Tong, L.; Kim, S.B.; Eisenach, L.; Valle, A.W.; Hardee, D.; Gordon, R.G.; Aziz, M.J. Alkaline quinone flow battery. *Science* **2015**, *349*, 1529–1532. [CrossRef] [PubMed]
76. Wang, W.; Xu, W.; Cosimbescu, L.; Choi, D.; Li, L.; Yang, Z. Anthraquinone with tailored structure for a nonaqueous metal-organic redox flow battery. *Chem. Commun.* **2012**, *48*, 6669–6671. [CrossRef] [PubMed]
77. Brushett, F.R.; Vaughey, J.T.; Jansen, A.N. An All-Organic Non-aqueous Lithium-Ion Redox Flow Battery. *Adv. Energy Mater.* **2012**, *2*, 1390–1396. [CrossRef]
78. Matsunaga, T.; Kubota, T.; Sugimoto, T.; Satoh, M. High-performance Lithium Secondary Batteries Using Cathode Active Materials of Triquinoxalinylenes Exhibiting Six Electron Migration. *Chem. Lett.* **2011**, *40*, 750–752. [CrossRef]

79. Huang, J.; Cheng, L.; Assary, R.S.; Wang, P.; Xue, Z.; Burrell, A.K.; Curtiss, L.A.; Zhang, L. Liquid Catholyte Molecules for Nonaqueous Redox Flow Batteries. *Adv. Energy Mater.* **2014**, *5*. [CrossRef]
80. Kaur, A.P.; Holubowitch, N.E.; Ergun, S.; Elliott, C.F.; Odom, S.A. A Highly Soluble Organic Catholyte for Non-Aqueous Redox Flow Batteries. *Energy Technol.* **2015**, *3*, 476–480. [CrossRef]
81. Wei, X.; Xu, W.; Huang, J.; Zhang, L.; Walter, E.; Lawrence, C.; Vijayakumar, M.; Henderson, W.A.; Liu, T.; Cosimbescu, L.; *et al*. Radical Compatibility with Nonaqueous Electrolytes and Its Impact on an All-Organic Redox Flow Battery. *Angew. Chem. Int. Ed. Engl.* **2015**, *54*, 8684–8687. [CrossRef] [PubMed]
82. Nakahara, K.; Oyaizu, K.; Nishide, H. Organic Radical Battery Approaching Practical Use. *Chem. Lett.* **2011**, *40*, 222–227. [CrossRef]
83. Nakahara, K.; Iwasa, S.; Satoh, M.; Morioka, Y.; Iriyama, J.; Suguro, M.; Hasegawa, E. Rechargeable batteries with organic radical cathodes. *Chem. Phys. Lett.* **2002**, *359*, 351–354. [CrossRef]
84. Bergner, B.J.; Schurmann, A.; Peppler, K.; Garsuch, A.; Janek, J. TEMPO: A mobile catalyst for rechargeable Li-O(2) batteries. *J. Am. Chem. Soc.* **2014**, *136*, 15054–15064. [CrossRef] [PubMed]
85. Shiga, T.; Hase, Y.; Yagi, Y.; Takahashi, N.; Takechi, K. Catalytic Cycle Employing a TEMPO–Anion Complex to Obtain a Secondary Mg–$O_2$Battery. *J. Phys. Chem. Lett.* **2014**, *5*, 1648–1652. [CrossRef] [PubMed]
86. Moshurchak, L.M.; Buhrmester, C.; Wang, R.L.; Dahn, J.R. Comparative studies of three redox shuttle molecule classes for overcharge protection of $LiFePO_4$-based Li-ion cells. *Electrochim. Acta* **2007**, *52*, 3779–3784. [CrossRef]
87. Taggougui, M.; Carré, B.; Willmann, P.; Lemordant, D. Application of a nitroxide radical as overcharge protection in rechargeable lithium batteries. *J. Power Sources* **2007**, *174*, 643–647. [CrossRef]
88. Wei, X.; Xu, W.; Vijayakumar, M.; Cosimbescu, L.; Liu, T.; Sprenkle, V.; Wang, W. TEMPO-Based Catholyte for High-Energy Density Nonaqueous Redox Flow Batteries. *Adv. Mater.* **2014**, *26*, 7649–7653. [CrossRef] [PubMed]
89. Takechi, K.; Kato, Y.; Hase, Y. A Highly Concentrated Catholyte Based on a Solvate Ionic Liquid for Rechargeable Flow Batteries. *Adv. Mater.* **2015**, *27*, 2501–2506. [CrossRef] [PubMed]
90. Kolosnitsyn, V.S.; Karaseva, E.V. Lithium-sulfur batteries: Problems and solutions. *Russ. J. Electrochem.* **2008**, *44*, 506–509. [CrossRef]
91. Price, A.; Bartley, S.; Male, S.; Cooley, G. A novel approach to utility-scale energy storage. *Power Eng. J.* **1999**, *13*, 122–129. [CrossRef]
92. Remick, R.; Ang, P. Electrically Rechargeable Anionically Active Reduction-Oxidation Electrical Storage-Supply System. *U.S. Patent* 4485154, 27 November 1984.
93. Szanto, D.A. Characterisation of Electrochemical Filter-Press Reactors. Ph.D. Thesis, University of Portsmouth, Portsmouth, UK, 1999.
94. Pan, H.; Wei, X.; Henderson, W.A.; Shao, Y.; Chen, J.; Bhattacharya, P.; Xiao, J.; Liu, J. On the Way Toward Understanding Solution Chemistry of Lithium Polysulfides for High Energy Li-S Redox Flow Batteries. *Adv. Energy Mater.* **2015**, *5*. [CrossRef]
95. Yang, Y.; Zheng, G.; Cui, Y. A membrane-free lithium/polysulfide semi-liquid battery for large-scale energy storage. *Energy Environ. Sci.* **2013**, *6*, 1552–1558. [CrossRef]
96. Lowe, M.A.; Gao, J.; Abruna, H.D. Mechanistic insights into operational lithium-sulfur batteries by *in situ* X-ray diffraction and absorption spectroscopy. *RSC Adv.* **2014**, *4*, 18347–18353. [CrossRef]
97. Kim, J.-H.; Kim, K.J.; Park, M.-S.; Lee, N.J.; Hwang, U.; Kim, H.; Kim, Y.-J. Development of metal-based electrodes for non-aqueous redox flow batteries. *Electrochem. Commun.* **2011**, *13*, 997–1000. [CrossRef]
98. Ding, F.; Xu, W.; Graff, G.L.; Zhang, J.; Sushko, M.L.; Chen, X.; Shao, Y.; Engelhard, M.H.; Nie, Z.; Xiao, J.; *et al*. Dendrite-free lithium deposition via self-healing electrostatic shield mechanism. *J. Am. Chem. Soc.* **2013**, *135*, 4450–4456. [CrossRef] [PubMed]
99. Lu, Y.; Goodenough, J.B. Rechargeable alkali-ion cathode-flow battery. *J. Mater. Chem.* **2011**, *21*, 10113–10117. [CrossRef]
100. Lu, Y.; Goodenough, J.B.; Kim, Y. Aqueous cathode for next-generation alkali-ion batteries. *J. Am. Chem. Soc.* **2011**, *133*, 5756–5759. [CrossRef] [PubMed]
101. Bauer, I.; Thieme, S.; Brückner, J.; Althues, H.; Kaskel, S. Reduced polysulfide shuttle in lithium–sulfur batteries using Nafion-based separators. *J. Power Sources* **2014**, *251*, 417–422. [CrossRef]
102. Ding, Y.; Zhao, Y.; Yu, G. A Membrane-Free Ferrocene-Based High-Rate Semiliquid Battery. *Nano Lett.* **2015**, *15*, 4108–4113. [CrossRef] [PubMed]

103. Zhao, Y.; Ding, Y.; Song, J.; Peng, L.; Goodenough, J.B.; Yu, G. A reversible $Br_2/Br^-$ redox couple in the aqueous phase as a high-performance catholyte for alkali-ion batteries. *Energy Environ. Sci.* **2014**, *7*, 1990–1995. [CrossRef]
104. Zhao, Y.; Byon, H.R. High-Performance Lithium-Iodine Flow Battery. *Adv. Energy Mater.* **2013**, *3*, 1630–1635. [CrossRef]
105. Zhao, Y.; Hong, M.; Bonnet Mercier, N.; Yu, G.; Choi, H.C.; Byon, H.R. A 3.5 V lithium-iodine hybrid redox battery with vertically aligned carbon nanotube current collector. *Nano Lett.* **2014**, *14*, 1085–1092. [CrossRef] [PubMed]
106. Zhao, Y.; Wang, L.; Byon, H.R. High-performance rechargeable lithium-iodine batteries using triiodide/iodide redox couples in an aqueous cathode. *Nat. Commun.* **2013**, *4*. [CrossRef] [PubMed]
107. Duduta, M.; Ho, B.; Wood, V.C.; Limthongkul, P.; Brunini, V.E.; Carter, W.C.; Chiang, Y.-M. Semi-Solid Lithium Rechargeable Flow Battery. *Adv. Energy Mater.* **2011**, *1*, 511–516. [CrossRef]
108. Hamelet, S.; Larcher, D.; Dupont, L.; Tarascon, J.M. Silicon-Based Non Aqueous Anolyte for Li Redox-Flow Batteries. *J. Electrochem. Soc.* **2013**, *160*, A516–A520. [CrossRef]
109. Fan, F.Y.; Woodford, W.H.; Li, Z.; Baram, N.; Smith, K.C.; Helal, A.; McKinley, G.H.; Carter, W.C.; Chiang, Y.M. Polysulfide flow batteries enabled by percolating nanoscale conductor networks. *Nano Lett.* **2014**, *14*, 2210–2218. [CrossRef] [PubMed]
110. Chen, H.; Zou, Q.; Liang, Z.; Liu, H.; Li, Q.; Lu, Y.C. Sulphur-impregnated flow cathode to enable high-energy-density lithium flow batteries. *Nature Commun.* **2015**, *6*. [CrossRef] [PubMed]
111. Ventosa, E.; Buchholz, D.; Klink, S.; Flox, C.; Chagas, L.G.; Vaalma, C.; Schuhmann, W.; Passerini, S.; Morante, J.R. Non-aqueous semi-solid flow battery based on Na-ion chemistry. P2-type $Na_xNi_{0.22}Co_{0.11}Mn_{0.66}O_2$-$NaTi_2(PO_4)_3$. *Chem. Commun.* **2015**, *51*, 7298–7301. [CrossRef] [PubMed]
112. Li, Z.; Smith, K.C.; Dong, Y.; Baram, N.; Fan, F.Y.; Xie, J.; Limthongkul, P.; Carter, W.C.; Chiang, Y.M. Aqueous semi-solid flow cell: Demonstration and analysis. *Phys. Chem. Chem. Phys.* **2013**, *15*, 15833–15839. [CrossRef] [PubMed]
113. Janoschka, T.; Martin, N.; Martin, U.; Friebe, C.; Morgenstern, S.; Hiller, H.; Hager, M.D.; Schubert, U.S. An aqueous, polymer-based redox-flow battery using non-corrosive, safe, and low-cost materials. *Nature* **2015**, *527*, 78–81. [CrossRef] [PubMed]
114. Wei, T.-S.; Fan, F.Y.; Helal, A.; Smith, K.C.; McKinley, G.H.; Chiang, Y.-M.; Lewis, J.A. Biphasic Electrode Suspensions for Li-Ion Semi-solid Flow Cells with High Energy Density, Fast Charge Transport, and Low-Dissipation Flow. *Adv. Energy Mater.* **2015**, *5*. [CrossRef]
115. Wang, Q.; Zakeeruddin, S.M.; Wang, D.; Exnar, I.; Gratzel, M. Redox targeting of insulating electrode materials: A new approach to high-energy-density batteries. *Angew. Chem. Int. Ed. Engl.* **2006**, *45*, 8197–8200. [CrossRef] [PubMed]
116. Huang, Q.; Li, H.; Gratzel, M.; Wang, Q. Reversible chemical delithiation/lithiation of $LiFePO_4$: Towards a redox flow lithium-ion battery. *Phys. Chem. Chem. Phys.* **2013**, *15*, 1793–1797. [CrossRef] [PubMed]
117. Pan, F.; Yang, J.; Huang, Q.; Wang, X.; Huang, H.; Wang, Q. Redox Targeting of Anatase $TiO_2$ for Redox Flow Lithium-Ion Batteries. *Adv. Energy Mater.* **2014**, *4*. [CrossRef]